Available online at www.sciencedirect.com
SCIENCE DIRECT
Pergamon
Cement and Concrete Research 34 (2004) 1633–1644
CEMENT AND CONCRETE RESEARCH

Composition and microstructural changes of cement pastes upon heating, as studied by neutron diffraction

Marta Castellote[a,*], Cruz Alonso[a], Carmen Andrade[a], Xavier Turrillas[a,b], Javier Campo[c]

[a]*Institute of Construction Sciences "Eduardo Torroja", CSIC, 28033, Madrid, Spain*
[b]*European Synchrotron Radiation Facility (ESRF), Grenoble, France*
[c]*Institute Laue Langevin (ILL), Grenoble, France*

Received 4 January 2002; accepted 8 July 2003

Abstract

Composition and microstructure changes of cement pastes when heating until 620 °C and cooling afterwards have been monitored on site by neutron diffraction. The parameters involved in the study have been the heating ramp, the state of the sample (in block or ground) and the type of cement. The residual state of the samples has also been studied by mercury intrusion porosimetry (MIP) and thermogravimetry analysis (TGA). As a result, it has been possible to monitor the major features of the experiments, i.e., the phases existence domains and their growing and decaying for portlandite, ettringite, calcite, lime, larnite, and hydrated calcium silicate (CSH gel), as well as the loss of free and bounded water during the experiments. In addition, the different residual phases in the matrix depending on the experimental set up have been established, which might have a significant influence in the durability of a concrete after a fire.

Keywords: Heating; In situ neutron diffraction; Microstructure changes; Cement paste; Fire simulation

1. Introduction

When a hardened concrete is exposed to high temperatures or to the direct action of a fire, physical and chemical transformations take place which lead to an important loss of mechanical strength of the material. Generally, it is accepted that the compressive strengths of an unprotected gravel type concrete decrease abruptly when reaching temperatures above 300 °C [1].

Some research on the behaviour of concrete submitted to high temperatures have been focused in studying the alterations of the mechanical properties (compressive strength, elastic limit, fluency resistance, etc. [2–5]. Other studies have been devoted to the changes of the physical properties (thermal conductivity, expansion, porosity, etc.) [6,7]. Numerical studies have been carried out for predicting the processes that take place [8], and also some references have been found on the chemical changes that occur in the bulk of the concrete [8] or in the simultaneous study of the physical–chemical alterations [9–13]. However, there is still a lack of knowledge concerning the basic mechanisms of the microstructural changes induced by the increase of temperature beyond the ordinary ones.

Even thought on-site dehydration of hydrated calcium silicate minerals has been reported in literature [14], no references have been found for the on-site monitoring of the changes that take place in the phase composition of cement pastes when heating, which is the contribution reported in this paper. Experiments of heating (up to 620 °C and subsequent cooling) cement pastes, in different conditions, with simultaneous neutron diffraction data acquisition have been carried out.

The crystalline phases in a sample can be studied using diffraction techniques, preferably with an intense incident beam; such is the case of synchrotron X-ray or neutron sources. Both approaches are complementary. Synchrotron light can help to acquire, if necessary, diffraction patterns in a few milliseconds. However, the diffracting volume analysed is very small and it might happen that the observations are not statistically representative of the whole. Neutron diffraction techniques overcome this problem as neutrons can penetrate deep into materials in a nondestructive way, so, they are very useful tools to understand how the material changes and degrade by providing information about the

* Corresponding author. Tel.: +34-91-3020440; fax: +34-91-3020700.
E-mail address: martaca@ietcc.csic.es (M. Castellote).

0008-8846/$ – see front matter © 2003 Elsevier Ltd. All rights reserved.
doi:10.1016/S0008-8846(03)00229-1

Table 1
Chemical composition (in %) of the cements used

Cement	SO_3	SiO_2	Al_2O_3	Fe_2O_3	CaO	MgO	Na_2O	K_2O	L of I	I R
A	3.23	18.78	5.63	3.05	62.86	1.78	0.18	1.00	3.45	1.97
B	3.89	19.89	3.05	4.12	63.71	1.55	0.13	0.45	1.53	1.92

Table 2
Conditions for the experiments performed

	Exp-1	Exp-2	Exp-3	Exp-4
Cement	A	A	A	B
Ramp of heating (°C/h)	60	120	120	60
Ramp of cooling (°C/h)	natural	natural	natural	natural
Sample	block	block	powder	block

bulk of the samples. In addition, they are scattered by all elements, also the light ones like the hydrogen isotopes; thus, information on moisture or hydrated elements can also be obtained. For these reasons neutron diffraction has been chosen as the technique of this investigation.

The correlation between these in situ studies and the residual state of the treated specimens, analysed by mercury intrusion porosimetry (MIP) and thermogravimetry analysis (TGA), has allowed to improve the understanding of the fundamentals of the processes.

2. Experimental

2.1. Materials and preparation of specimens

Two series of cement pastes with w/c = 0.45 were prepared; both using deuterated water from Merck of 99.95% purity.

The first series was prepared using ordinary Portland cement, with high C_3A content (>9%) and high alkaline content (>0.84% Na_2O eq.), which is named as cement A. The second series was made with ordinary Portland cement, with low C_3A content (< 1%) and low alkaline content (< 0.43 Na_2O eq.) (cement B), whose compositions are given in Table 1.

The specimens were cast in plastic tubes of 8 mm diameter and 40 mm in height which were sealed and

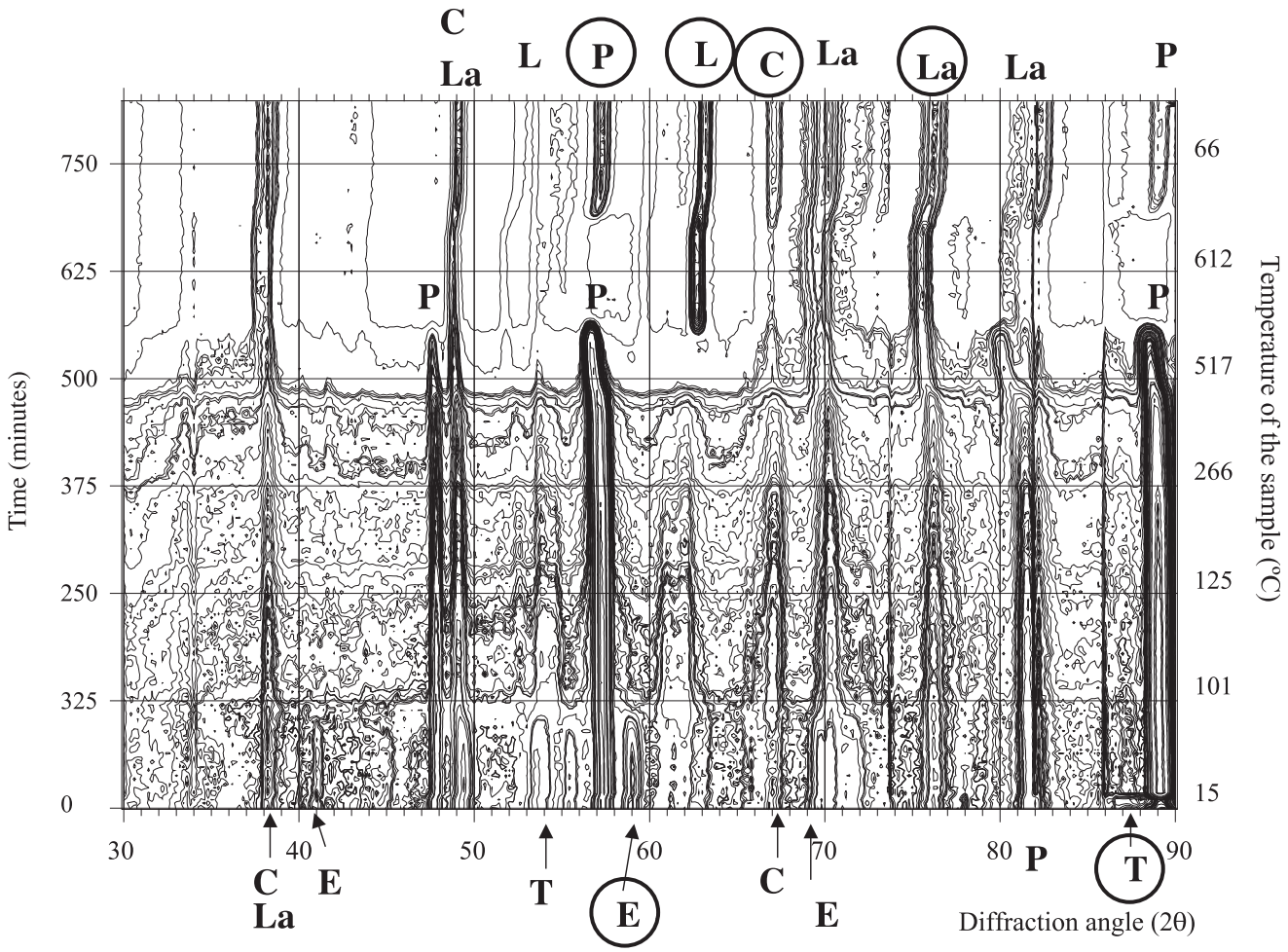

Fig. 1. Thermodiffractometry contour map of the experiment labelled as exp-1 (block of paste, cement A and heating rate of 60 °C/h). Meaning of the letters P: portlandite, E: ettringite, C: calcite, L: lime, T: CSH gel, La: larnite. Marked with a circle the reflexions specified in Table 3.

isolated from the atmosphere during 28 days, until tested. In addition, a thermocouple of K-type was embedded in every sample when casting to monitor the actual temperature of the specimens during the experiments.

2.2. Techniques and procedures

The experiments of heating (up to 620 °C and subsequent cooling) with simultaneous diffraction data acquisition, were performed in the D1B instrument of the Institute Max von Laue—Paul Langevin (ILL), in Grenoble, France. This is a high-flux two-axes diffractometer coupled to a multidetector with 400 cells encompassing 80° in 2θ. The wavelength used was 2.5253 Å, and the sample holder (a tube of quartz) was introduced in a furnace with control K-type thermocouples. The temperature was regulated within an accuracy of ± 1 °C.

Four experiments were performed in air atmosphere. Three of them on samples cast with the cement named as cement A in Table 1, and the last one with cement B. The variables involved in the study have been the heating ramp, the state of the sample (in a block or ground) and the type of cement. The conditions for the four experiments are given in Table 2.

Neutron diffraction data were collected continuously storing the detector counts every 300 s, exploring an angular domain in 2θ from 10° to 90°.

Two weeks after the neutron experiments took place, a portion of the samples tested in exp-1, exp-3 and exp-4, as well as untreated samples, cast with the two cements, were analysed by TGA and MIP to study the residual state of the specimens. TGA analysis were performed in a NETZSCH STA 409 C equipment, with a heating rate of 4 K/min until reaching 1050 °C, in N_2 atmosphere. For the MIP, a Micromeritics Porosimeter was employed. The value used for the contact angle was 130° with a penetrometer constant of 10.79 μL/pF.

3. Results

3.1. Neutron diffraction patterns

In Figs. 1–4, contour maps for the diffraction data are sketched. In these figures, data are displayed as the

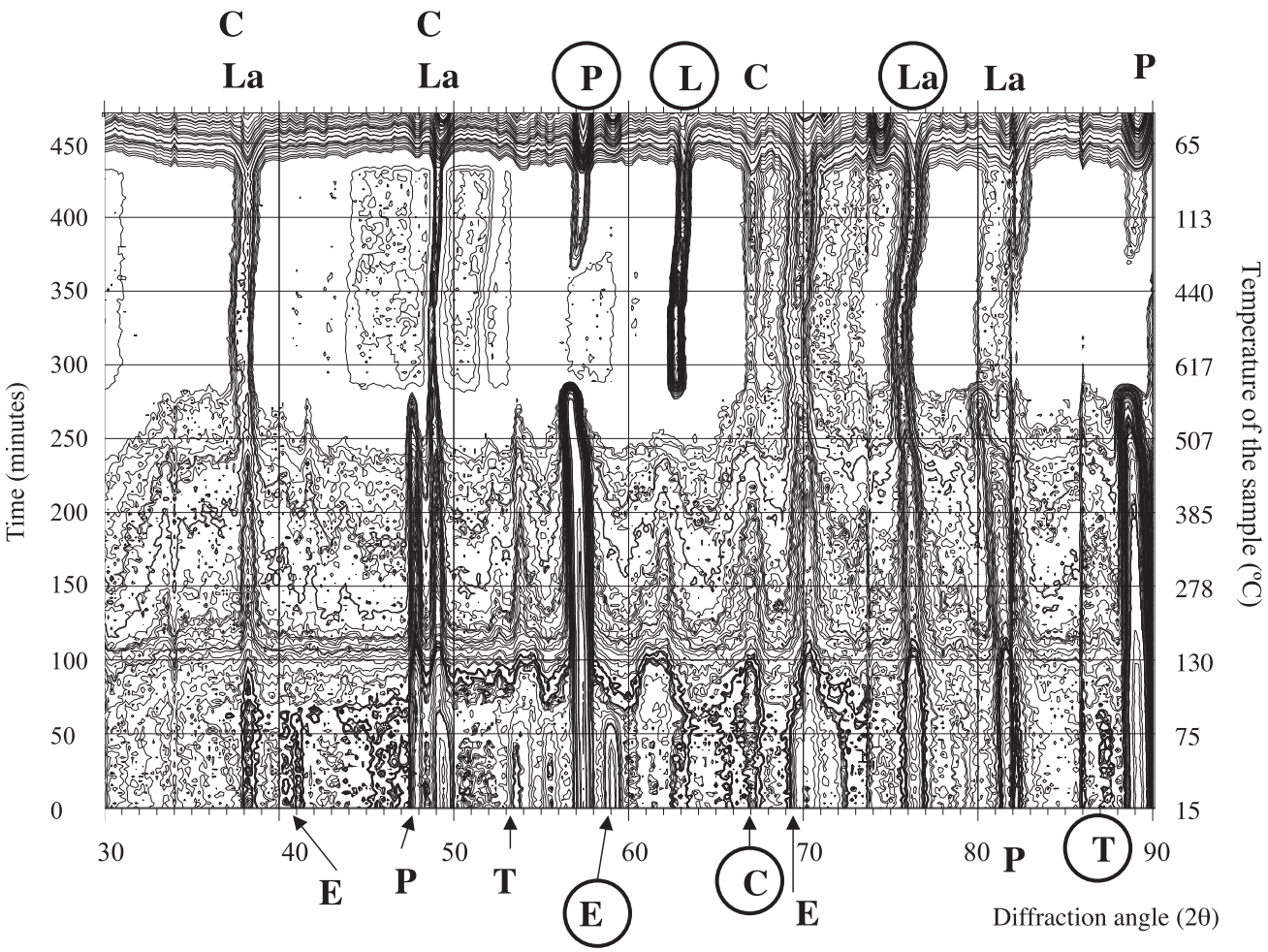

Fig. 2. Thermodiffractometry contour map of the experiment labelled as exp-2 (block of paste, cement A and heating rate of 120 °C/h). Meaning of the letters P: portlandite, E: ettringite, C: calcite, L: lime, T:CSH gel, La: larnite. Marked with a circle the reflexions specified in Table 3.

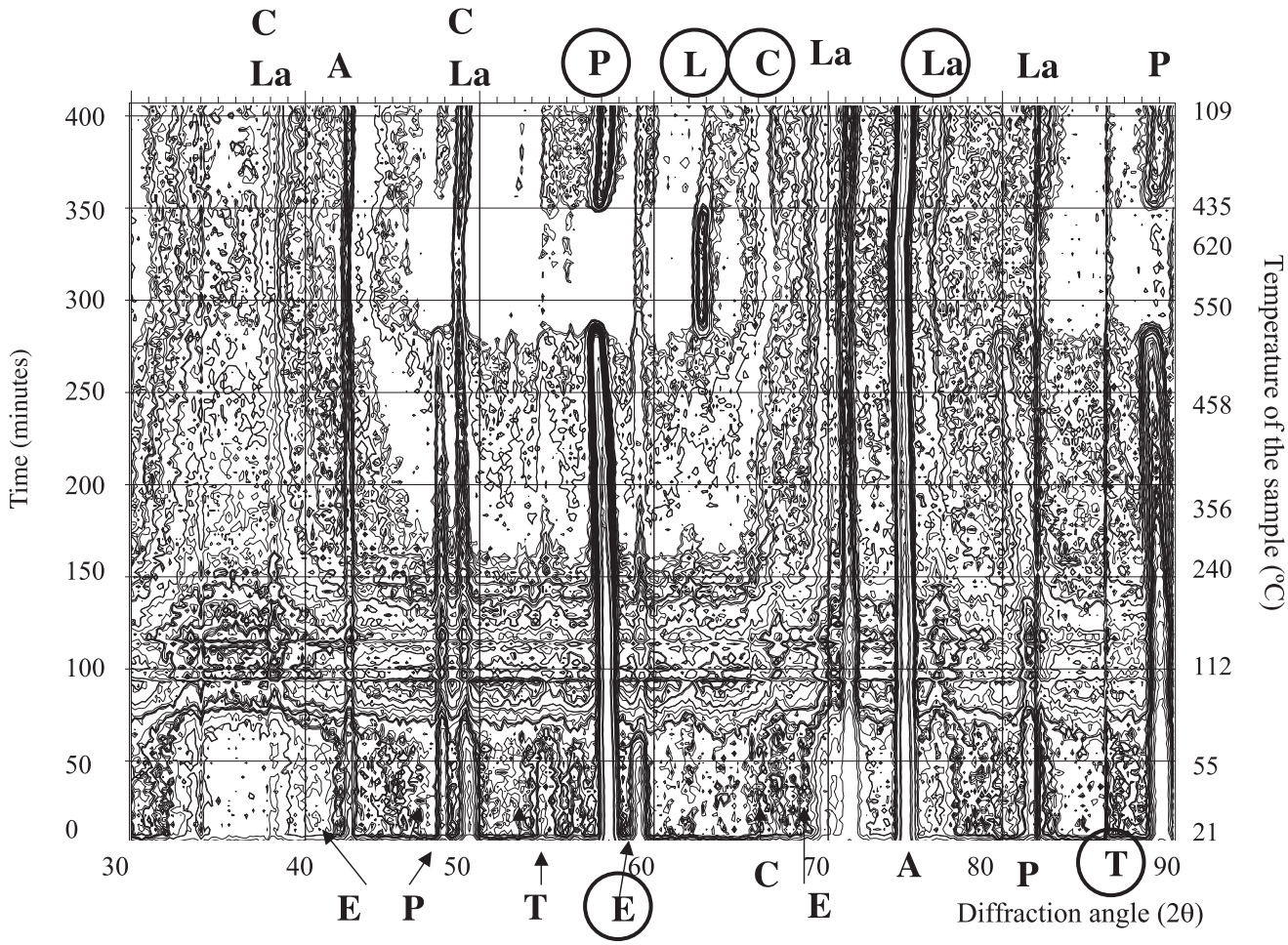

Fig. 3. Thermodiffractometry contour map of the experiment labelled as exp-3 (powdered sample, cement B and heating rate of 120 °C/h). Meaning of the letters P: portlandite, E: ettringite, C: calcite, L: lime, T: CSH gel, La: larnite, A: Al_2O_3 tube. Marked with a circle the reflexions specified in Table 3.

projection (in the 2θ-time plane) of a pseudo three-dimensional map obtained after sequentially connecting the diffraction patterns. The resulting plots are contour maps allowing the observation of the major features of the whole experiments, i.e., the phases existence domains and their growing and decaying. On the left axis, the time of the experiment is represented, while on the right axis the corresponding internal temperature is given.

The analysis of the these neutron diffraction patterns has allowed the identification of six main crystal phases: portlandite, ettringite, calcite, lime, hydrated calcium silicate (CSH gel) and larnite. Some of the peaks corresponding to each phase are marked in Figs. 1–4.

As an example, to clarify the meaning of Figs. 1–4, in Fig. 5, a zoom of Fig. 3, covering the interval 55–64° in 2θ, is given in the form of a surface plot. In it, some peaks corresponding to portlandite, ettringite, lime and CSH, as well as their evolution, are clearly shown.

Selected peaks of these phases, which are given in Table 3, were chosen by their isolation and intensity and they were fitted to Gaussian curves for the whole series. This was done with procedures written in IDL code using the Marquart algorithm. The variation of intensity of a chosen reflection for a particular phase along the experiment (related with the concentration) was used to monitor concentration changes. Similarly the shifts of reflection positions (related with cell expansion) as well as the full width at half maximum (FWHM; related with crystallinity and the size of grain) of the fitted Gaussians were determined.

The peaks, whose evolution has been analysed, have the corresponding Miller indices presented in Table 3. In Figs. 1–4 these peaks have been marked with circles around the letter identifying each phase.

It has to be remarked that, as exp-3 was made on a powdered sample, the wire of the thermocouple was introduced in a capillary tube of Al_2O_3 to make it rigid and avoid any movement during the experiment. Therefore, two intense peaks, corresponding to this phase, appear in Fig. 3 that are not relevant for the experiment as Al_2O_3 is an inert material at the temperature of the experiment.

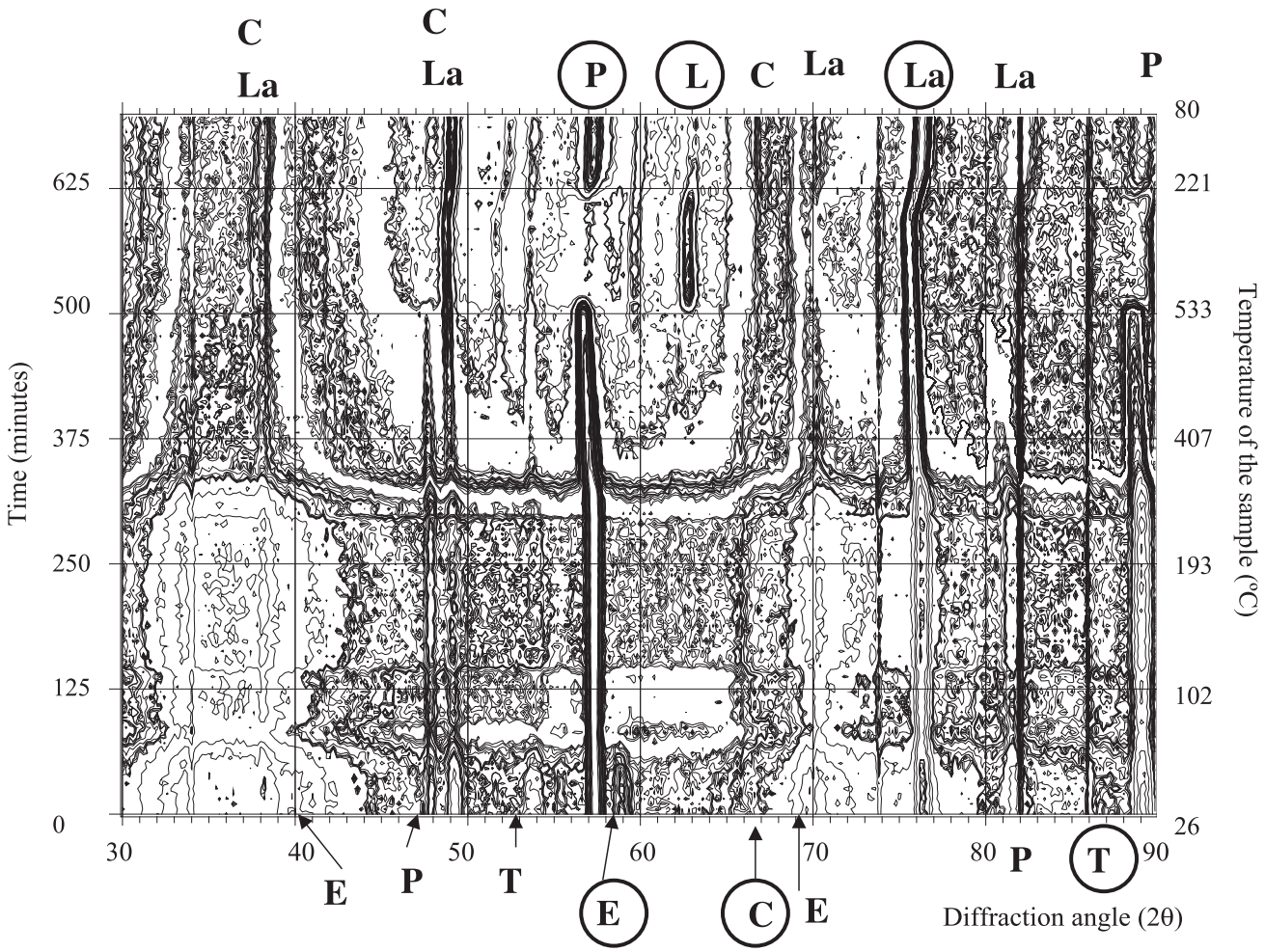

Fig. 4. Thermodiffractometry contour map of the experiment labelled as exp-4 (block of paste, cement B and heating rate of 60 °C/h). Meaning of the letters P: portlandite, E: ettringite, C: calcite, L: lime, T: CSH gel, La: larnite. Marked with a circle the reflexions specified in Table 3.

A more detailed analysis of the evolution of the concentration of these crystalline phases with temperature are presented in Fig. 6a–f, where the evolution of the normalised intensity as a function of the internal temperature of the specimen (°C) for the six peaks analysed is depicted. Heating is represented by dark symbols while cooling is given as empty ones.

3.1.1. Evolution of the intensities (related to the concentration of the different phases)

Fig. 6 shows that during heating up to 100 °C, intensity of portlandite and calcite increase due to precipitation caused by the loss of the free water in the pores of the paste. Furthermore, there is an additional release of Ca^{2+} coming from the decomposition of ettringite (completely disappeared by 90 °C), which certainly contributes to the precipitation of both portlandite and calcite. This behaviour cannot be noticed in exp-3 with powdered sample, whose intensity decreases in the very beginning of the experiment. This is attributed to a very quick initial carbonation of the powder, as can be deduced from the increase of calcite in the same region of temperature (Fig. 6d). When reaching an internal temperature that depending on the experiment ranges between 530 °C (exp-3 and exp-4) and 560 °C (exp-1 and exp-2), portlandite decomposes abruptly, being transformed into lime (Fig. 6c).

The peak corresponding to the CSH gel, presents quite high dispersion, being the general tendency for all the experiments a slight decrease as it gets dehydrating, having disappeared completely at 400 °C for the block samples. For the powdered sample, not crystalline CSH gel was detected beyond 200 °C. Part of the CSH that decomposes contributes to increase the concentration of calcite (which remains during all the experiment, with little loss of CO_2, as their thermal decomposition temperature is about 700 °C) and larnite, whose previous hydration had formed the CSH gel.

During cooling, provided that the sample is not sealed, uptake of water vapour from the atmosphere takes place, which induces decomposition of CaO. In the case of exp-1 and exp-2, only part of it decomposes to form portlandite and larnite, while the decomposition is total in the case of

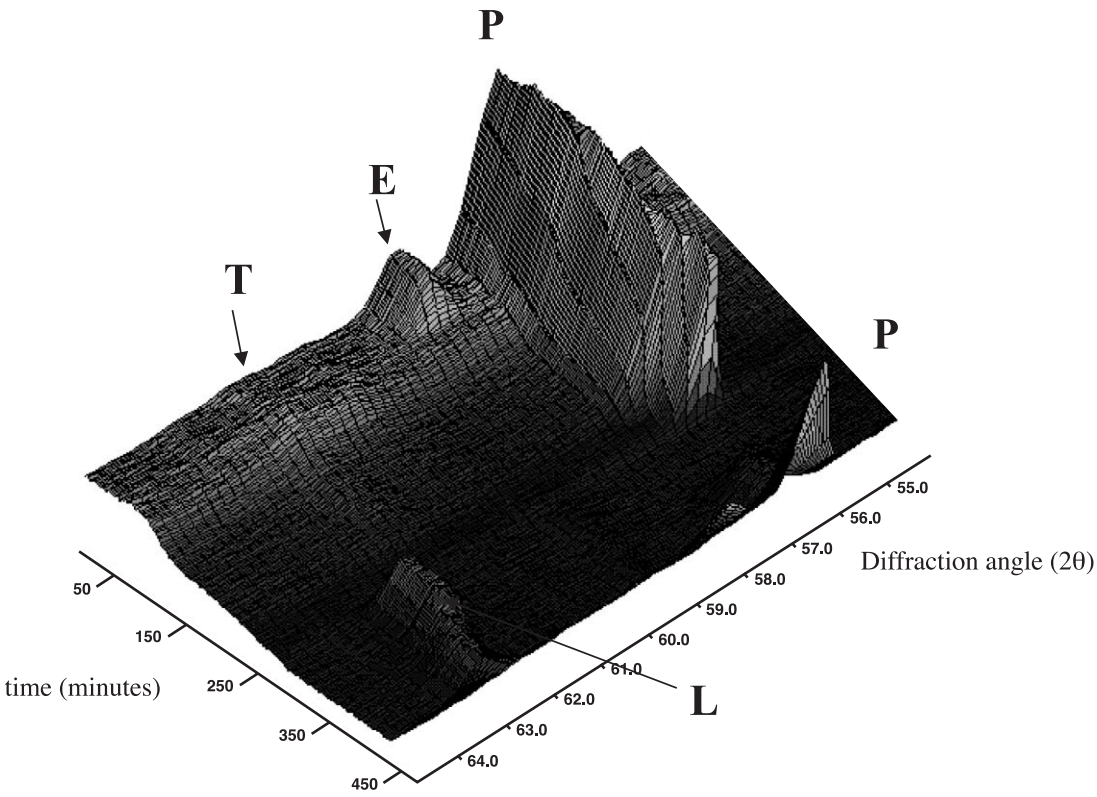

Fig. 5. Surface plot of the experiment labelled as exp-3 (powdered sample, cement B and heating rate of 120 °C/h) covering the interval 55–64° in 2θ. Meaning of the letters P: portlandite, E: ettringite, L: lime, T: CSH gel.

the powdered sample and when casting with cement B. Concerning ettringite and CSH gel, they are not recovered after cooling (see Fig. 6), while calcite uptakes CO_2 and reaches its maximum.

3.1.2. Evolution of the cell parameters of the different phases

In Fig. 7, the d-spacing (Å) of each diffraction peak has been represented. In it, it is shown that when temperature increases, an expansion of the unit cell takes place, as expected. It has to be noticed that the actual cell volumes cannot be calculated as not enough isolated peaks are available to compute the volumes, but the evolution of the d-spacing can be qualitatively assimilated to the evolution of the volume of the unit cell.

Table 3
Identification of the phases and of the plane corresponding to each peak analysed (h k l)

Name	Formula	Reference	Reflexion
Portlandite	$Ca(OH)_2$	[15]	(1 0 1)
Ettringite	$Ca_6(Al(OH)_6)_2(SO_4)_3(H_2O)_{26}$	[16]	(2 1 6)
Calcite	$CaCO_3$	[17]	(1 1 3)
Lime	CaO	[18]	(2 0 0)
Larnite	Ca_2SiO_4	[19]	(1 3 1)
CSH	(CaO)x(SiO2)y.z(H_2O)	[20]	(0 2 0)

Fig. 7a shows that in the case of portlandite, there is a point in which the slope of the increase rises noticeably. This point is different for the two cements tested, about 170 °C for cement A and 300° for cement B. Concerning the remaining size of the unit cell, after the experiments, it recovers the initial value. In the case of ettringite, it expands greatly when heating. In this case, there is also a difference between the two cements: the d-spacing is higher when ettringite is formed from a low C_3A cement (cement B), which is attributed to the fact of being ettringite a crystal structure very tolerant to variations of constituent ions.

On the contrary, the unit cell of lime is very similar for the four experiments, exhibiting a completely linear expansion with temperature. The case of calcite is different, and it is not very clear in Fig. 7d, as the d-spacing of each sample presents some variations. However, in all the experiments the trend is the same: There is an initial increase in the size of the cell, and when a certain precipitation takes place at about 100 °C, it starts to decrease steadily up to reaching a certain value (depending on the experiment) about 300–400 °C. After that point, it increases steadily. This behaviour might be related to the precipitation of calcite from the decomposition of other phases. The same could be attributed to larnite, which exhibits an important change of slope in

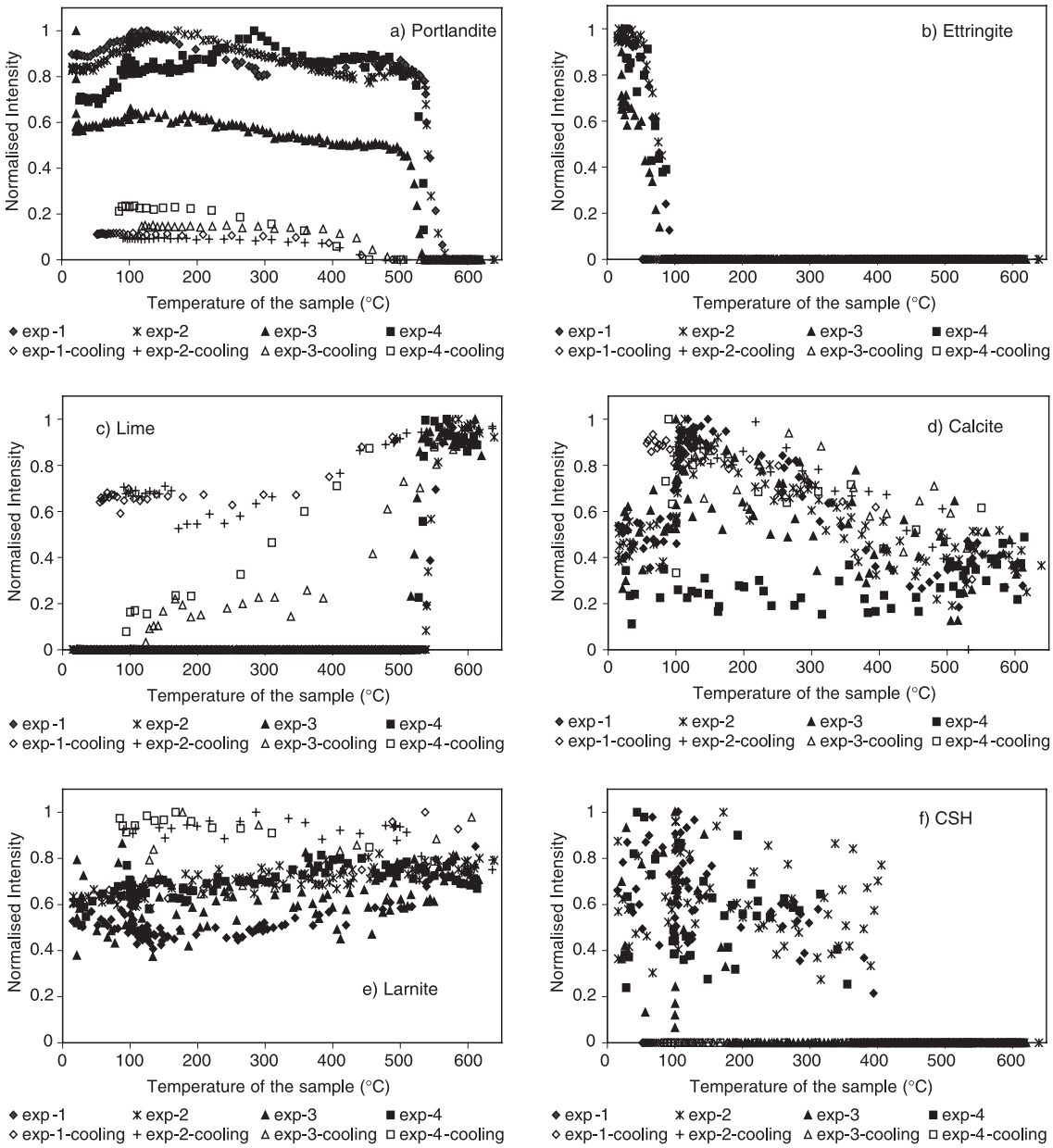

Fig. 6. Evolution of the normalised intensity for the six peaks analysed corresponding to (a) portlandite, (b) ettringite, (c) lime, (d) calcite, (e) larnite and (f) CSH gel.

the increasing trend in agreement with the disappearance of the CSH gel.

3.1.3. Evolution of the crystallinity degree

In Fig. 8, the FWHM of the portlandite has been represented. This parameter is related to crystal size: the smaller the FWHM of the peaks, the larger are the crystallites of the phase, or better the crystallinity degree. This parameter presents a clear trend only for portlandite. From the variation in the FWHM, it can be deduced that the one which is formed during the process of cooling, is by far less crystalline than the original one.

3.1.4. Dehydration during the heating process

Integration of the diffraction patterns backgrounds as a function of the internal temperature of the samples (normalised intensity to unity at the low 2θ region, where no peaks appear) is presented in Fig. 9. This parameter is related to the water (hydrogen) fraction in the sample, not only free water, but also combined water in the hydrates. So, it can be observed that the background decreases during heating, more quickly in the case of powdered samples, than when the specimen is heated in a block (compare exp-2 and exp-3). When increasing the ramp of heating, the combined water is lost at lower temperature (compare exp-1 and exp-2). In addition, different

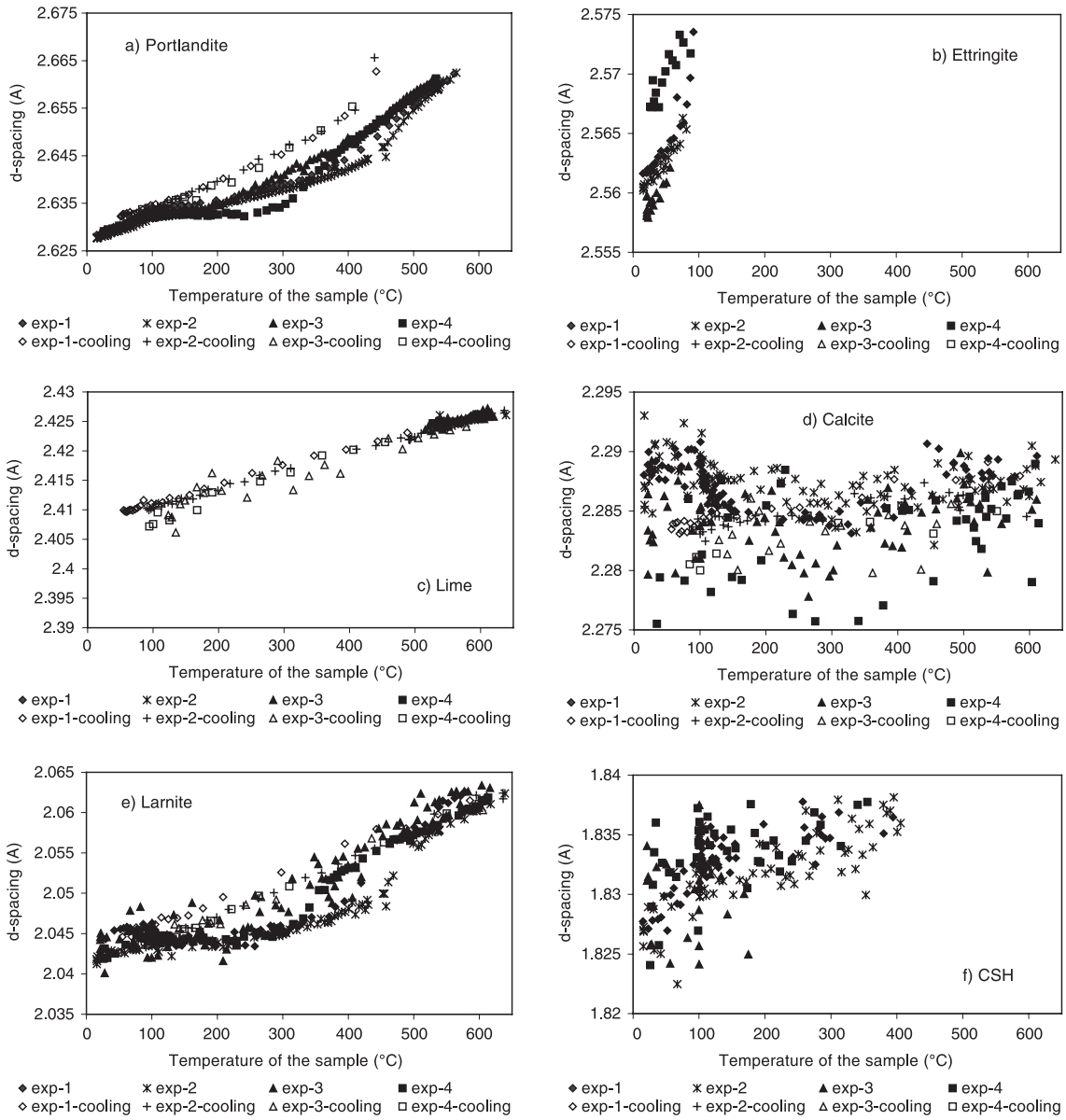

Fig. 7. Evolution of the d-spacing (Å) for the six peaks analysed corresponding to (a) portlandite, (b) ettringite, (c) lime, (d) calcite, (e) larnite and (f) CSH gel.

kind of cements leads to a different loss of water (compare exp-1 and exp-4). From Fig. 9 it can also be deduced than when cooling, no rehydration of the sample takes place, and CSH gel is not formed any more in these conditions.

3.2. Mercury intrusion porosimetry

The results obtained from MIP for the initial samples (with the two cements) and for the specimens submitted to exp-1, exp-3 and exp-4 are presented in Table 4, where the total porosity (percent in volume) and the density of the matrix are given.

In Table 4, it can be noticed that the heating treatment induces in all the samples an increase in the total porosity. A more detailed analysis can be made by looking at the differential pore size distributions for the different samples, as presented in Fig. 10.

Fig. 10 shows that the amount of pores higher than 10 μm is very high for the specimens after exp-3 and exp-4. As this range of pores cannot be considered very significant; the analysis has to be focused on the pores smaller than 10 μm. Concerning the different type of cements, both initial samples presented quite the same porosity distribution, showing two maxima around 1 and 0.1 μm. After exp-1, the capillary porosity has increased remarkably but showing two maxima at the same position than before the experiment. However, in the case of exp-3, it has produced a shift in the position of the maximum towards higher pore diameters, mainly be-

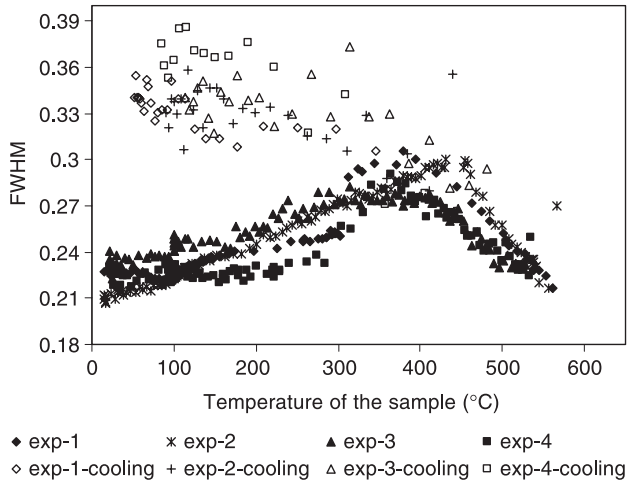

Fig. 8. Evolution of the FWHM for portlandite during the four experiments.

tween 1 and 10 μm, having lower porosity than the initial one in the low pores (0.1–0.01 μm). The same distribution has been found after exp-4, with a broad increase in the bigger capillary pores while decreasing the smallest ones.

3.3. Thermogravimetry analysis

The results obtained from TGA for the initial samples (with the two cements) and for the specimens submitted to exp-1, exp-3 and exp-4, are presented in Fig. 11, where the loss of mass (in percentage to the weight of sample) are depicted. From this figure, in accordance with the deductions from Fig. 6, it can be said that at long term, the CSH gel has not been recovered in any proportion. In addition, from the two steps (at 400 and 600 °C), changes in temperature of decomposition as well as the changes in the residual percentages of portlandite and calcite respectively, can be calculated. It

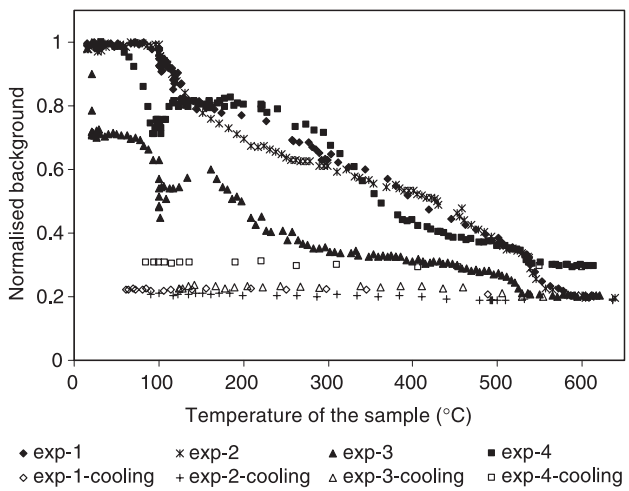

Fig. 9. Evolution of the background, at low 2θ, during the experiments.

Table 4
MIP microstructure parameters of the samples

	Exp-1 Sample		Exp-3 Sample		Exp-4 Sample	
	Before	After	Before	After	Before	After
Porosity (vol.%)	24.46	48.04	24.46	31.02	20.79	31.75
Density (g/cm^3)	1.6725	1.4754	1.6725	0.911	1.7967	0.87

is necessary to take into account that these values are relative, as they are percentages of the actual composition, which varies during the test. They are given in Table 5.

It can be observed in Table 5 that a permanent loss in the percentage of portlandite has been produced after every experiment, especially in the case of exp-4. As long as calcite is concerned, in the samples fabricated with cement A (with high C_3A content) the percentage is smaller than in the untreated sample. However, an increase in the residual

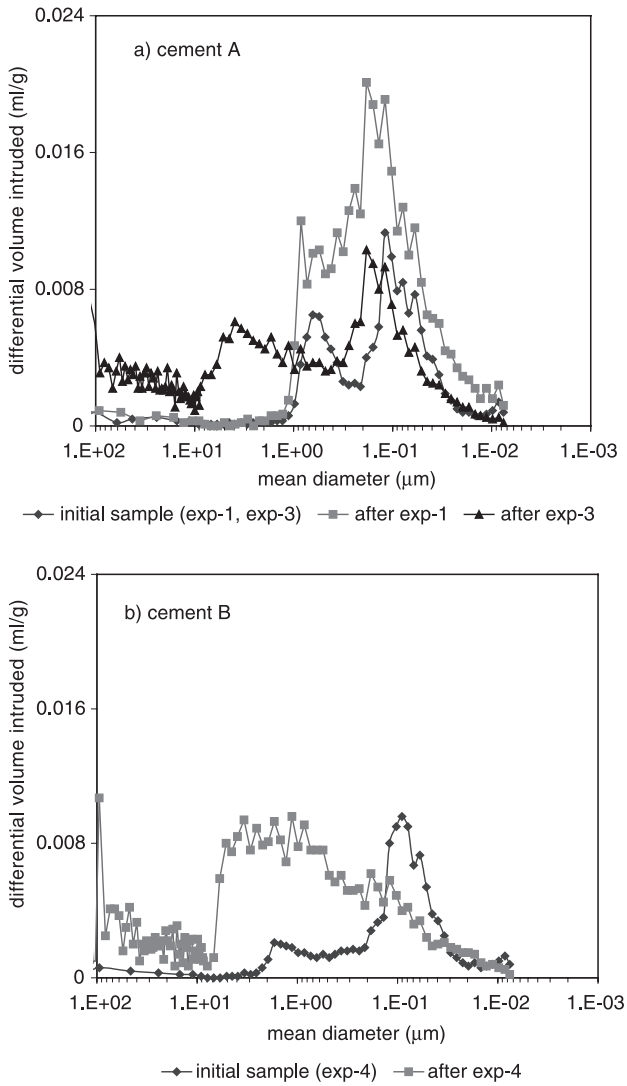

Fig. 10. Differential pore size distribution of the samples. (a) cement A. (b) cement B.

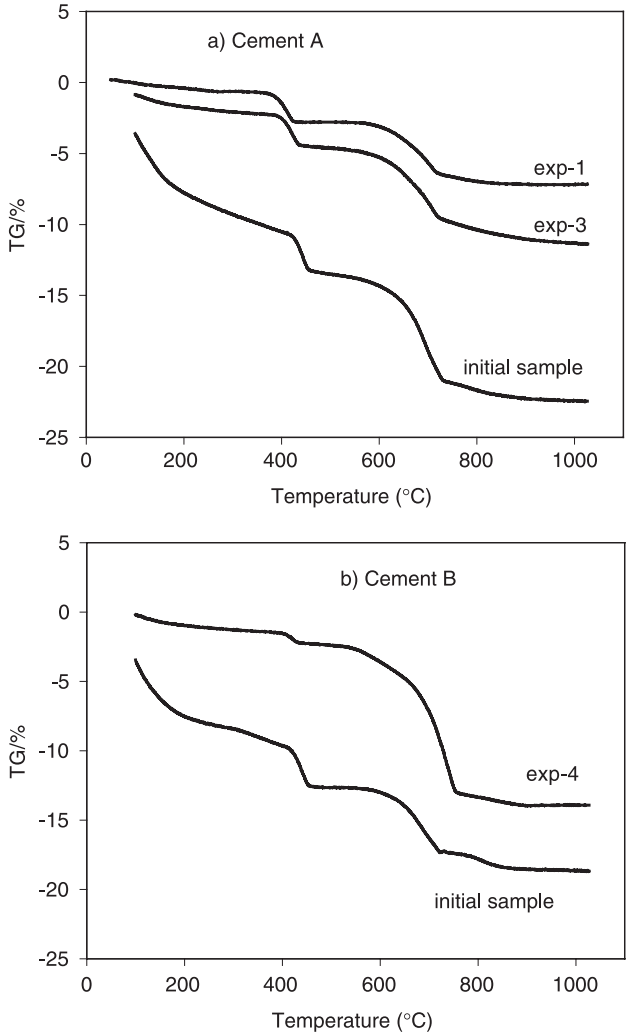

Fig. 11. TGA of the samples. (a) cement A. (b) cement B.

calcite after exp-4 with cement B (low C_3A content) has been produced.

Concerning the temperature of thermal decomposition, it is noticeable that the portlandite formed after cooling decomposes at lower temperature than the initial one, just on the opposite than calcite, which decomposes at higher temperature. This might be attributed to the poorer crystalline degree of the newly formed portlandite, as can be seen in Fig. 8, even though in the case of calcite this argument does not apply so clearly.

Table 5
Percentages of portlandite and calcite, and respective decomposition temperature, before and as residual state after the experiments

		Exp-1 Sample		Exp-3 Sample		Exp-4 Sample	
		Before	After	Before	After	Before	After
Portlandite	(%)	12.3	8.5	12.3	9.4	12.3	3.2
	Temperature	446	413.9	446	425.2	443.2	420.9
Calcite	(%)	14.7	4.8	14.7	7.3	8.45	19.25
	Temperature	687.0	695.5	687.0	701.2	679.1	731.4

4. Discussion

4.1. Calculation of the amount of portlandite and calcite lost in the experiments

Even though most of the TGA data in the literature are given as percentages of the sample weight, as long as the data are relative to the actual composition, which changes during heating, from the direct data of the TGA, it is not possible to know if it has produced a loss or gain of mass for a specific phase. Therefore, it has been considered necessary the calculation of the loss or gain of portlandite and calcite in absolute terms. To do so, the densities of the samples before and after the treatments were used to calculate the loss of mass, and the percentage of loss of each phase are given in Table 6.

Data in Table 6 can be deduced such that the residual composition is quite different when casting with the two different cements. The amount of residual portlandite has decreased in all the samples reaching an 87% of loss in the specimen cast with low C_3A cement (exp-4). Special mention can be made to the calcite, which has decreased in about a 70% after exp-1 and exp-2 while increased in absolute term up to a 10% after exp-4.

4.2. Influence of the heating conditions

First of all, it is necessary to point out that these four experiments do not cover the whole range of combinations of cement type, heating rate and sample form. However, for the conditions studied in present research, it can be deduced that the heating rate, in the range tested here (comparison between exp-1 and exp-2), has no significant influence in the resulting microstructure changes of cement paste. The only difference noticed was a faster dehydration of the CSH gel, in the range between 140 and 400 °C, temperature at which they behave again in the same manner.

On the contrary, as expected, heating the sample in block or as powder implies important differences (comparison between exp-2 and exp-3), which can be attributed to the ability to release the water vapour and the gases generated when heating. Therefore, in the powdered specimen, dehydration is much faster, with the signal corresponding to the crystal phases of the CSH gel disappearing at about 200 °C, in agreement with the evolution of the background for this experiment (see Fig. 8), whose trend is concave (while it is convex for the block samples). In addition, the temperature for decomposition of portlandite changes as well, being a

Table 6
Percentage of decrease in the amount of portlandite and calcite after the experiments (heating + cooling)

	Exp-1		Exp-3		Exp-4	
	Portlandite	Calcite	Portlandite	Calcite	Portlandite	Calcite
% Decrease	38.4	71.0	58.1	72.84	87.3	− 10.25

5% lower in the case of powdered sample. But the differences are not only related to the heating process; when cooling the block sample, only part of the CaO reacts to form portlandite and larnite, while the reaction is total in the case of the powdered sample.

Concerning the resulting microstructure, in the case of the block sample, together with the loss of material (portlandite, CSH, ettringite, calcite), the lack of ability to eliminate the water vapour of the block sample, implies the accumulation of tensions in the sample, which leads to the generalised increase in the capillary porosity in the range 0.01–1 μm, having an increase of 96.5% in the total porosity. In the case of the powdered sample (exp-3), the increase in the porosity is related to the loss of material [12], showing a decrease in the pore range <0.01 μm due to the dehydration of the CSH gel, as previously reported by the authors [11], and providing a distribution of the porosity with no massive increase in the capillary range of porosity.

The type of cement is the most influencing factor (comparison between exp-1 and exp-4). On one hand, loss of free water takes place faster in the case of the low C_3A content cement (exp-4), having lost all of it when reaching 95 °C. From that point, the loss of water is smaller than in the case of the high C_3A cement, until reaching 330 °C, where an inflexion point takes place because of the loss of the CSH gel, as can be seen in Fig. 4. However, in the case of the high C_3A cement (exp-1), the loss of water takes place steadily until about 500 °C. Changing the type of cement also changes the temperature for decomposition of portlandite, as well as their evolution of the d-spacing (Å) with the temperature. When cooling the samples, decomposition of the CaO formed when heating, with the sample in a block, is total in the low C_3A cement, while a large part of it remains in the high C_3A cement (see Fig. 6). This difference in the residual state (free lime content) might have influence from a durability point of view in a real structure after a fire.

The comparison of the behaviour of these two types of cements can be clearly observed in Figs. 12 and 13, where

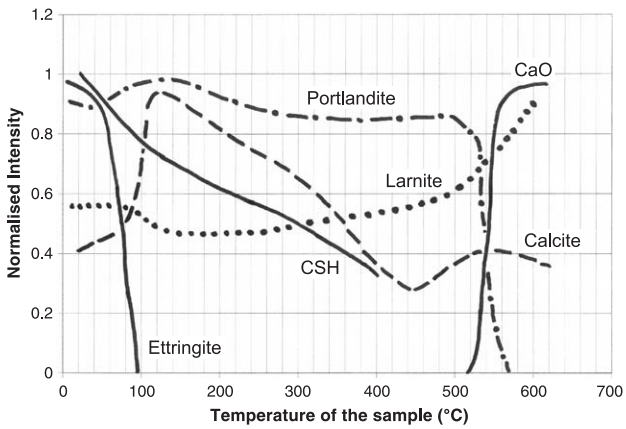

Fig. 12. Evolution of the normalised intensity during heating (exp-1) for the different phases analysed. Cement A.

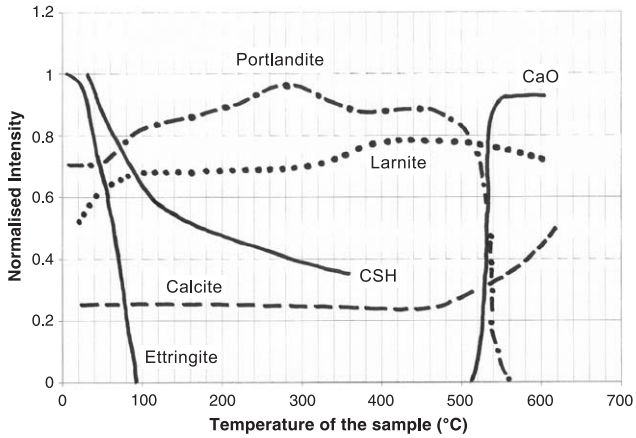

Fig. 13. Evolution of the normalised intensity during heating (exp-4) for the different phases analysed. Cement B.

the trends of the different phases, while heating during the same experiment, have been depicted for exp-1 and exp-4, respectively.

The increase or decrease of the intensity of each phase is related, as said previously, with its concentration, or more precisely, to the mass fraction of the phase with respect to the total crystalline amount. Provided that during this experiment there is a loss of material, an increase, therefore, in a peak can be due to either an increase in the concentration or a loss of mass in the sample, as calculated from the ATD data. Always taking this point into account, from Figs. 12 and 13, it can be noticed that calcite exhibits a different behaviour in the case of the two cements tested. In both cases, there is an increase of calcite and larnite when the crystalline fraction of the CSH gel disappears. It seems to imply that a decalcification of the CSH gel takes place. The released calcium, provided that the heating takes place in an open system, (with CO_2 available), might react to form calcite.

On the other hand, the decomposition of various type of CSH gel to give anhydrous phases had been reported in literature [2,14], which is in accordance with the results in present research. However, the mechanisms involved in these transformations are not completely understood from present results, and further research is being carried out by the authors.

Concerning the residual porosity there are also differences: The sample with low alkaline and C_3A content cement shows an important decrease in the range between 0.1 and 0.3 μm which might be attributed to the precipitation of calcite, which increased in absolute value after the experiment.

5. Conclusions

In this paper, composition and microstructural changes of cement pastes when heating until 620 °C and cooling

afterwards, has been monitored in situ by neutron diffraction, and the conclusions that can be drawn up are the following:

1. With these experiments it has been possible to monitor the major features of the experiments, i.e., the phases existence domains and their growing and decaying: when portlandite, present at the beginning, reaches an internal temperature (between 530 and 560 °C), it decomposes abruptly, being transformed into lime. Ettringite, which was present at the beginning in all the specimens, thermally decomposes when it reached 90 °C. The CSH gel slightly decreases as it gets dehydrated, disappearing at a temperature which depends on the dehydration of the gel (between 200 and 450 °C). Part of the CSH that decomposes seems to contribute to increase the concentration of calcite and larnite (both remained during all time of the experiments).
2. During cooling, uptake of water vapour from the atmosphere takes place, which induces reaction of CaO, to form portlandite. Depending on the experiment (powdered sample and when casting with low alkaline and C_3A content cement), the disappearance of the free lime is partial or total. Ettringite and CSH gel are not recovered during cooling while calcite uptakes CO_2 and reaches its maximum.
3. Portlandite that was formed when cooling is less crystalline than the original one, and its temperature of thermal decomposition gets lower. On the contrary, calcite that precipitates decomposes thermally at higher temperature than the original one.
4. The monitoring of the loss of free and combined water, by integration of diffraction patterns backgrounds as a function of the internal temperature of the samples has been related to the resulting microstructure: The lack of ability of the block samples to eliminate the water vapour implies the accumulation of tensions in the sample, which seems to lead to a generalised increase in the capillary porosity while in the case of the powdered sample, the increase in the porosity is attributed only to the loss of material.
5. Changing the heating rate, from 60 to 120 °C/h has no significant influence neither in the composition nor in the resulting microstructure of the cement paste; however, the type of cement or the state of the sample (powder or block) is a significant parameter, leading to different residual phases (free lime content), which might have a significant influence in the durability of a concrete after a fire.

Acknowledgements

The authors are grateful to Pierre Convert, A. Daramsy and J. Torregrossa for their help. The experiments were done and thanks is due to beamtime (Exp 5-25-39) granted by the Institut Max von Laue-Paul Langevin (ILL).

References

[1] G.A. Khoury, Compressive strength of concrete at high temperatures: a reassessment, Mag. Concr. Res. 44 (161) (1992) 291–309.
[2] Z.P. Bazant, M.F. Kaplan, Concrete at High Temperatures; Material Properties and Mathematical Models, Longman Group, England, 1996 (ISBN 0-582-08624-4).
[3] X. Fu, D.D.L. Chung, Reversible decrease of the flexural dynamic modulus of cement pastes up on heating, Cem. Concr. Res. 27 (6) (1997) 839–844.
[4] H.L. Malhotra, The effect of temperature on compressive strength of concrete, Mag. Concr. Res. (1956) 875–894.
[5] G.A. Koury, R. Sarshar, P.J.E. Sullivan, B.N. Grainger, Factors affecting the compressive strength of unsealed cement paste and concrete at elevated temperatures up to 600 °C, Wiss. Z. Hochsch. Archit. Bauwes. Weimar, B 36 (1–2) (1990) 89–92.
[6] F.S. Rostasy, C. Ehm, K. Hinrishsmeyer, Structural alterations in concrete due to thermal and mechanical stresses, in: J.C. Maso (Ed.), Pore Structure and Materials Properties, vol. 1, Chapman & Hall, London-New York, 1987, pp. 92–99.
[7] G.A. Koury, V.N. Grainger, P.J.E. Sullivan, Transient thermal strain of concrete: Literature review, conditions within specimen and behaviour of individuals constituents, Mag. Concr. Res. 37 (132) (1985 Sept.) 131–143.
[8] G.R. Consolazio, M.C. McVay, J.W. Rish, Measurement and prediction of pore pressures in saturated cement mortar subject to radiant heating, ACI Mater. J. 95 (5) (1998) 525–536.
[9] F.S. Rostasy, R. Weis, G. Wiedemann, Changes of pore structure of cement mortars due to temperature, Cem. Concr. Res. 10 (1980) 157–164.
[10] J. Piasta, Heat transformations of cement phases and the microstructure of cement paste, Mater. Const. 17 (102) (1984) 415–420.
[11] C. Alonso, C. Andrade, E. Menéndez, Evolución microestructural de hormigones de altas y ultra altas resistencias a elevadas temperaturas, Hormigōn y acero 221–222 (2001) 97–105.
[12] M. Heikal, Effect of temperature on the physico–mechanical and mineralogical properties of Homra pozzolanic cement pastes, Cem. Concr. Res. 30 (2000) 1835–1839.
[13] S.K. Handoo, S. Agarwal, S.K. Agarwal, Physicochemical, mineralogical and morphological characteristics of concrete exposed to elevated temperatures, Cem. Concr. Res. 32 (2002) 1009–1018.
[14] S. Shaw, C.M.B. Henderson, B.U. Komanschek, Dehydration/recrystallization mechanisms, energetics and kinetics of hydrated calcium silicate minerals: An in situ TGA/DSC and synchrotron radiation SAXS/WAXS study, Chem. Geol. 167 (2000) 141–159.
[15] O. Chaix-Pluchery, J. Pannetier, J. Bouillot, J.C. Niepce, Structural prereactional transformations in $Ca(OH)_2$, J. Solid State Chem. 67 (1987) 225–234.
[16] A.E. Moore, H.F.W. Taylor, Crystal structure of Ettringitte, Acta Crystallogr., B 26 (1970) 386–393.
[17] R. Wartchow, Data compilation obtained for calcite from the "learned profile method (LP)", and comparison with the "background peak background method (BPB)", Z. Kristallogr. 186 (1989) 300–302.
[18] Q. Huang, O. Chmaissem, J.J. Caponi, C. Chaillout, M. Marezio, J.L. Santoro, A. Santoro, Neutron powder diffraction study of the crystal structure of $HgBa_2Ca_4Cu_5O_{12}+d$ at room temperature and at 10 K, Physica C (1994) 1–9.
[19] T. Tsurumi, Y. Hirano, H. Kato, T. Kamiya, M. Daimon, Crystal structure and hydration of belite, CETRE 40 (1994) 19–25.
[20] S.A. Hamid, The crystal structure of the 11 Angs. Natural Tobermorite $Ca_{2.25}(Si_3O_{7.5}(OH)_{1.5})(H_2O)$, Z. Kristallogr. 154 (1981) 189–198.